Journal of Catalysis **187,** 167–176 (1999)
Article ID jcat.1999.2601, available online at http://www.idealibrary.com on IDEAL®

Hydroisomerization of Pentane, Hexane, and Heptane for Improving the Octane Number of Gasoline

A. Chica and A. Corma[1]

Instituto de Tecnología Química (UPV-CSIC), Universidad Politécnica de Valencia, Avenida los Naranjos, s/n, 46022 Valencia, Spain

Received March 9, 1999; revised June 9, 1999; accepted June 9, 1999

The hydroisomerization of *n*-heptane to dibranched and tribranched products for producing high octane gasoline has been studied using unidirectional 12 Membered Ring (MR) zeolites with different pore diameters, and zeolites with other pore topologies including one with connected 12 × 10 MR pores and two tridirectional 12 MR zeolites. Besides the pore topology, the crystallite size of the zeolite was seen to be of paramount importance for improving activity and selectivity. In a second part of the work, a Light Straight Run naphtha including *n*-pentane and *n*-hexane and another feed containing *n*-pentane, *n*-hexane, and *n*-heptane have been successfully isomerized using a nanocrystalline Beta (BEA) zeolite. This can be a favourable alternative to the commercial zeolite catalyst based on mordenite (MOR), especially when *n*-heptane is present in the feed.

Key Words: **paraffin isomerization; Light Straight Run isomerization; octane improvement of naphtha by paraffin isomerization; zeolite topology; crystal size for paraffin isomerization.**

1. INTRODUCTION

To increase the octane number of the gasoline pool, the Light Straight Run (LSR) gasoline fraction of oil is isomerized and in this way its Research Octane Number (RON) increases from ∼64 to ∼80. This increase is achieved by isomerizing *n*-pentane and *n*-hexane, which are the main components of LSR, to the corresponding isopentane and mono and dibranched hexanes which have higher octane number.

The commercial catalysts used for carrying out this isomerization are Pt on chlorinated alumina and Pt H-mordenite (1–4). The former is more active and allows one to perform the isomerization at lower temperatures (180°C) with the corresponding thermodynamic benefit on the equilibrium yield of branched products (Fig. 1). However, the major drawback of this catalyst is the sensitivity to water and sulfur even in concentrations as low as 10 ppm. On the other hand, Pt-mordenite requires higher reaction temperature (250°C) with the corresponding 2-point RON penalty, but with the advantage of being much more resistant to water and sulfur.

Recently, some units are processing LSR feeds in which the main component is *n*-hexane, followed by *n*-pentane, but they also contain nonnegligible amounts of *n*-heptane. It can be expected that a catalyst based on Pt/H-mordenite will be able to successfully perform the isomerization of *n*-hexane and *n*-pentane but will crack the *n*-heptane introduced to the reactor. Two main catalyst factors will contribute to the loss of *n*-heptane by cracking, the high acid strength of mordenite and the dimensions of the 12 MR pore with 0.65 nm diameter, which will strongly diminish the diffusion of di- and especially tribranched products out of the pores, giving these hydrocarbons the opportunity to crack.

In this work we have studied another zeolitic catalytic system and showed how the acidity, pore shape, and crystallite size of zeolites may influence the ratio of cracking to isomerization, as well as the distribution of the isomers obtained during the hydroisomerization of *n*-heptane. This has been investigated, on the one hand, to explore the possibilities of zeolites for the isomerization of *n*-heptane as a possible alternative to the reforming of this alkane to toluene and, on the other hand, with the objective of generating the basic information which will allow us to select new catalysts and to test them for the isomerization of LSR feed containing *n*-pentane, *n*-hexane, and *n*-heptane.

2. EXPERIMENTAL

Zeolites were studied with a system of 12 Membered Ring (MR) unidirectional channels with different dimensions (mordenite (MOR) and SSZ-24 (AFI)) and molecular sieves with similar pore dimensions and different compositions (SSZ-24 (AFI) and SAPO-5 (AFI)), together with zeolites containing interconnected 10 and 12 MR pores (SSZ-33(CON)), and 12 MR tridirectional zeolites (Y (FAU) and Beta (BEA)). The mordenite (MOR) catalyst was prepared starting with a commercial sample from PQ Corporation which was dealuminated by a combination of acid and

---

[1] To whom correspondence should be addressed. Fax: 34 96 3877809. E-mail: acorma@itq.upv.es.

0021-9517/99 $30.00

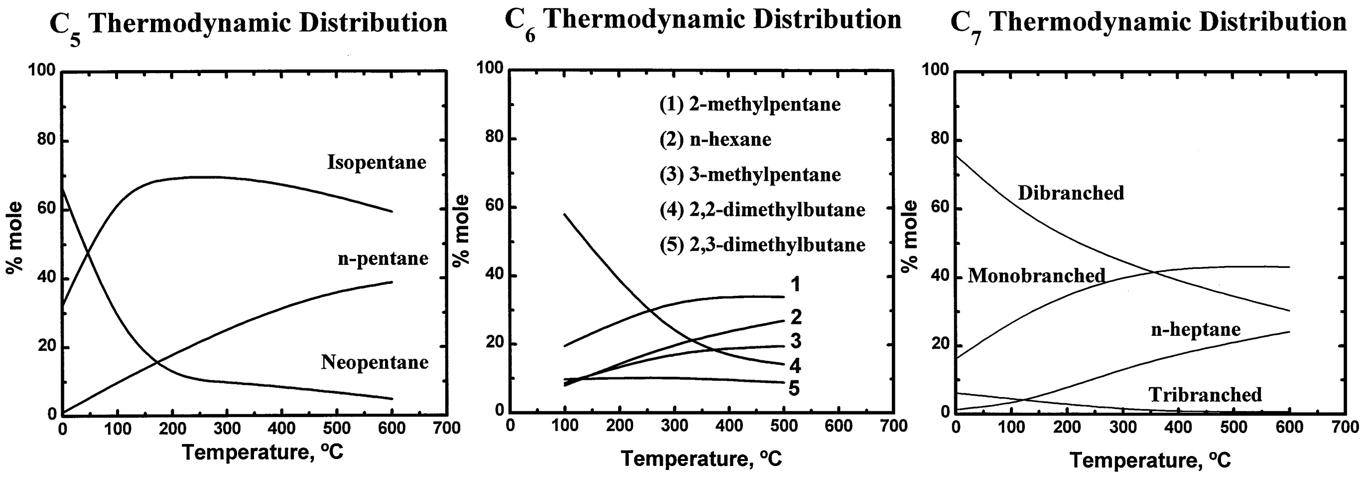

FIG. 1. Thermodynamic distribution of C_5, C_6, and C_7.

steam treatment following Refs. (5, 6). The SSZ-24 (AFI) sample was prepared following the procedure given in (7). SAPO-5 (AFI) was prepared following a modified procedure described in (8), and SSZ-33 (CON) was prepared following (9). Beta (BEA) samples with similar chemical compositions but different crystallite sizes were obtained from PQ Corporation (sample BetaPQ) and by synthesis (SCB (BEA) and LSC (BEA)) following the synthesis procedure reported before (10, 11). USY (FAU) samples (USY 720 and USY 760) with different framework compositions were obtained from PQ Corporation. Pt, 0.5wt%, was incorporated on all molecular sieve samples by pore volume impregnation with an aqueous solution of H_2PtCl_6 (6).

N_2 adsorption (BET), SEM (JOEL JSM 6300 Link Isis), pyridine adsorption–desorption (12), and ^{27}Al MAS NMR and ^{29}Si MAS NMR have been carried out in order to characterize the zeolite samples. Infrared spectroscopic measurements were carried out with a Nicolet 710 FTIR spectrometer. Wafers of 10 mg cm^{-2} were introduced into a conventional greaseless IR cell and pretreated in vacuum (10^{-2} Pa) at 400°C overnight. For adsorption/desorption pyridine studies 6.66.10^2 Pa pyridine was introduced into the cell at room temperature. After reaching equilibrium, the samples were outgassed at 250, 350, and 400°C under vacuum and the spectra were recorded at room temperature. Solid state ^{27}Al MAS NMR and ^{29}Si MAS NMR spectra were recorded at ambient temperature on a Varian VXR-400 Wb spectrometer at 104.2 and 79.5 MHz, respectively.

The catalytic experiments were conducted in a fully automated stainless steel fixed bed continuous reactor with an on-line analytical system (G.C. Varian 3400) equipped with a 50-m Petrocol DH50 column. The reaction conditions used in this work are 5.13 WHSV, H_2/hydrocarbon ratio of 15 mol mol^{-1}, 20 bar total pressure, and reaction temperatures ranging from 240 to 380°C.

3. RESULTS AND DISCUSSION

3.1. *Isomerization of n-Heptane*

The micropore volumes of the studied samples (Table 1) indicate that good crystalline samples have been produced. Concerning the chemical composition of the mordenite, it is known that the best LSR isomerization catalysts have a Si/Al ratio between 10 and 20 (13, 14). Due to the impossibility of preparing SSZ-24 with an Si/Al ratio in that range, we have studied two mordenite samples, one with the optimal (Si/Al = 17) and another with a Si/Al ratio close to that of SSZ-24. In an analogous way, two USY and two Beta samples with two levels of Si/Al ratio have been studied as well (see Table 1).

The crystallite size is another parameter which may have an important impact on product distribution. Thus, while we were not successful in producing all zeolite samples with the same crystallite size, we attempted to keep the average crystal size similar for all zeolites in each of the homogeneous series of catalysts (mordenite, SSZ-24 , SAPO-5 and Beta USY, SSZ-33) and at the same time to study the role of crystallite size in the isomerization activity and selectivity by changing the crystallite size of zeolite Beta in a wide range while keeping the chemical composition constant. It has to be noted that the Si/Al ratios in Table 1 correspond to the values determined by chemical analysis, except those for for USY zeolites in which the framework Si/Al ratio was calculated from the unit cell size parameter using the Fichtner–Sehmittler equation (15).

The Al^{27} MAS NMR results (spectra not shown) indicate that in all samples some dealumination has occurred during the activation process; together with framework Al (57 ppm), some extra-framework Al was present (0 ppm). Since owing to the presence of internal silanols Si(3Si, 1OH), it becomes difficult to calculate reliable framework

TABLE 1

Characteristics of Different Catalysts Used in Reaction

Catalyst	Si/Al	Pore vol. (cc/gr)	Crystal size (μm)	Brønsted (micromole py/gr cat.)				Lewis (micromole py/gr cat.)		
				150°C	250°C	350°C	400°C	150°C	250°C	350°C
MOR(17)(MOR)	17	0.109	1		43	24	7		24	24
SSZ-24(AFI)	50	0.12	1		25	19	6		46	34
SSZ-33(CON)	16	0.213	0.1		49	29	22		37	31
B-PQ(BEA)	16	0.189	0.15		46	26	15		48	36
USY-760(FAU)	55	0.203	0.4		14	3	1		10	7
USY-720(FAU)	30	0.203	0.4		54	27	11		13	12
SCB(BEA)	16	0.151	>0.030		39	16	10		60	46
LCB(BEA)	13	0.217	0.05 × 10		52	24	20		14	26
MOR(40)(MOR)	40	0.169	1		74	39	—		16	19
BETA(50)(BEA)	50	0.176	0.15		22	12	3		18	21
SAPO-5(AFI)	—	0.18	1	17	17	5		10	13	19

Si/Al ratios by Si^{29} MAS NMR on these zeolites, we have worked with the values given by the chemical analysis. Nevertheless, and since in the case of the isomerization of paraffins on well-balanced bifunctional and stable catalysts, as is our case (see Fig. 2), the controlling step is the Brønsted acid catalyzed reaction (16, 17), we have determined the acidity of the different zeolites by carrying out the adsorption of pyridine at room temperature and the desorption

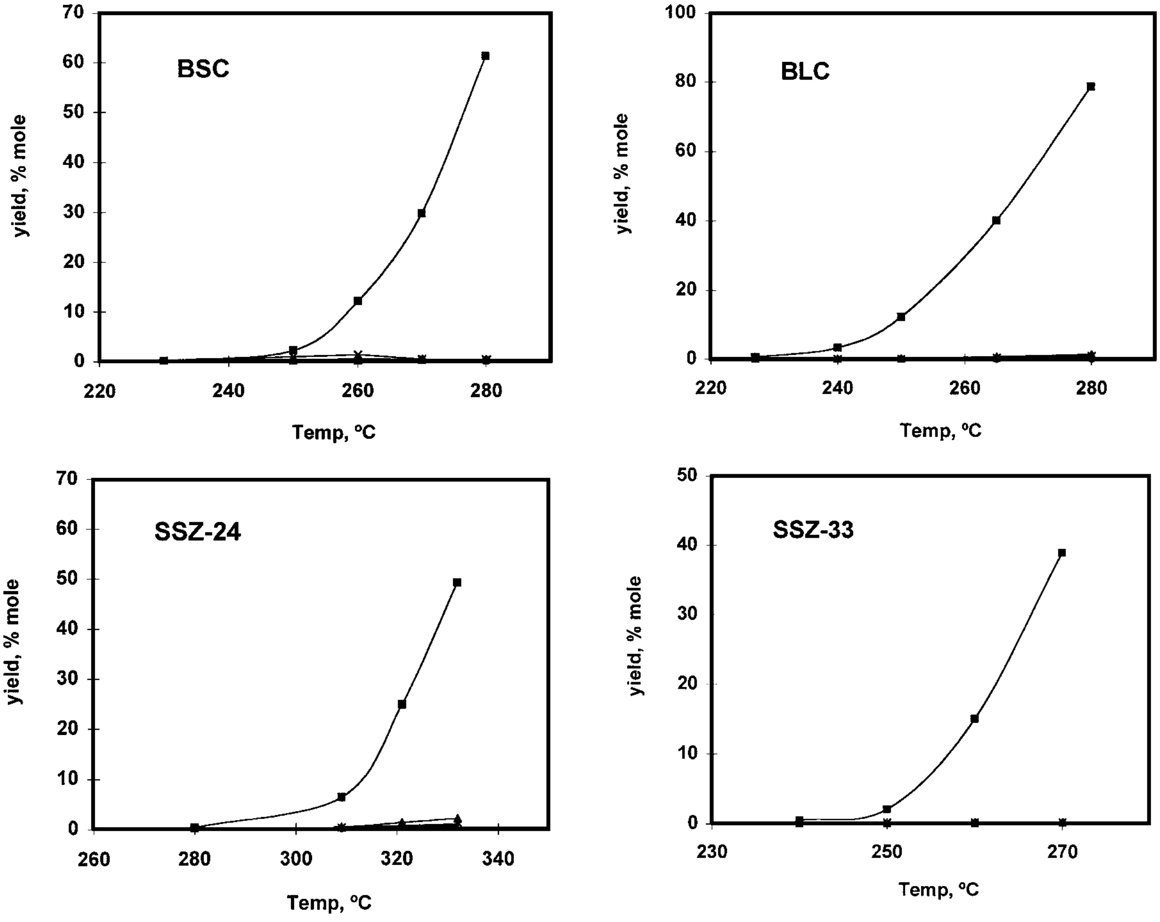

FIG. 2. Cracking product distribution in the isomerization of *n*-heptane over different catalysts: $C_1 + C_2$ (◆), $C_3 + C_4$ (■), C_5 (▲), and C_6 (×). Reaction conditions: 5.13 WHSV, 20 bar total pressure, and H_2/hydrocarbon ratio of 15 mol mol^{-1}.

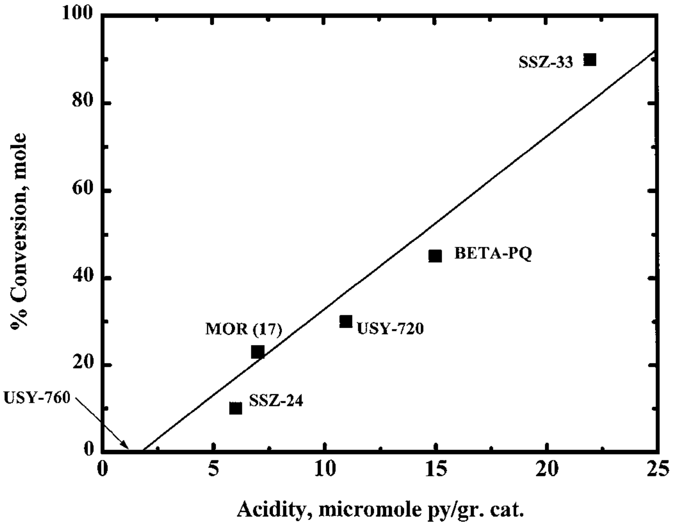

FIG. 3. Variation of the catalytic activity with the number of acid sites present on the catalyst, as measured by pyridine desorption at 400°C.

at 250, 350, and 400°C. The catalytic activity of the different catalysts was correlated with the number of acid sites measured by pyridine after 400°C desorption temperature, and a very good linear correlation is observed, regardless of the pore dimensions and chemical composition of the zeolite (Fig. 3). Among the different unidirectional structures studied, the one with a larger pore diameter (SSZ-24) gives better selectivities. This conclusion is valid regardless of the framework Si/Al ratio of the mordenite used. Indeed, even when a mordenite sample containing a higher Si/Al ratio was used as isomerization catalyst (Fig. 4b), the SSZ-24 structure with larger pore diameter still gave a better selectivity to branched products.

Since the pore size or, even better, the fast diffusion of the bulkier branched products out of the pores is an important parameter controlling the final catalyst selectivity, one should also consider large pore tridirectional zeolites as potential isomerization catalysts. Up to now the only large pore tridirectional structures known are Y and Beta zeolites. However, taking into account the catalytic behaviour of the tridirectional 10 × 12 MR SSZ-33 structure (18), this zeolite can also be a candidate for the isomerization of *n*-heptane. Figure 4a shows that its activity, as well as its isomerization selectivity, is better than that of SSZ-24, but worse than that of Beta and USY zeolites.

From the point of view of the octane number of the products produced, it is unfortunate that none of these zeolites is adequate for producing a high octane C_7 isomerate, since the isomers produced in larger amounts are the monomethyl isomers with little dimethylpentane and almost no trimethylbutane, which are the most interesting products (Figs. 5a and 5b).

When comparing the distribution of isomers obtained with that predicted by the thermodynamic equilibrium, it can be seen that both di- an trimethyl isomers are formed in amounts below the equilibrium distribution due to the very fast cracking of the dimethylpentane carbocation isomers which are depleted, enabling at the same time the formation of trimethylbutane. (19). Of course, in this case, the lower the pore diameter of the zeolite, the higher its tortuosity and acid strength, and the higher the number of acid sites with the same acid strength, the lower the selectivity to di- and trimethyl C_7 isomers will be. This can be observed when comparing the two USY zeolites with Si/Al ratios of 30 and 55. In both cases all Al atoms should be isolated, and therefore all the bridging hydroxyl groups should have the same acid strength. Thus the sample with a lower Si/Al ratio, and therefore with a larger number of acid sites, is more active but less selective for isomerization (Table 1 and Fig. 4b).

Another factor which is expected to have an influence on the branching isomerization selectivity is the zeolite crystallite size. This is so due to the fact that the smaller the crystallite sizes, the shorter the length of the pores will be and consequently the faster the diffusion of reactants and products will be. In order to study this, a nanocrystalline Beta sample (0.03 μm) was prepared following the procedure reported elsewhere (10). The nanocrystalline Beta zeolite has a lower thermal stability than Beta samples with a larger crystallite size, and this implies that more dealumination occurs during the activation process. This is reflected in a decrease of the acidity measured, which is lower for the nanocrystalline Beta than for the commercial Beta despite the higher Al content of the nanocrystalline sample. Nevertheless and despite the fact that the nanocrystalline Beta has a lower acidity, its activity is higher, and so is the selectivity for isomerization. On top of that, at the same level of conversion, the selectivity for dibranched and tribranched C_7 paraffins, even if it is still low, is higher on the nanocrystalline Beta zeolite (Fig. 5a). Moreover, on nanocrystalline Beta the dimethylpentanes with higher RON are favoured (see Fig. 6). When the results obtained on the nanocrystalline Beta are compared with those on the other zeolites studied here, it is clear that the former gives by far the best results. Based on this the nanocrystalline Beta zeolite can be considered as a potential LSR isomerization catalyst. In order to explore this possibility we have studied its catalytic properties for the isomerization of two LSR feeds, one feed rich in *n*-pentane that also contains *n*-hexane, and another enriched with *n*-hexane (60 wt%) and also containing *n*-pentane (20 wt%) and *n*-heptane (20 wt%).

3.2. LRS Isomerization on Nanocristalline Beta

The results presented in Fig. 7 clearly shows that when a simulated LSR feed containing *n*-pentane and *n*-hexane in an *n*-pentane/*n*-hexane molar ratio of 1.8 is reacted, nanocrystalline Beta zeolite is a highly selective

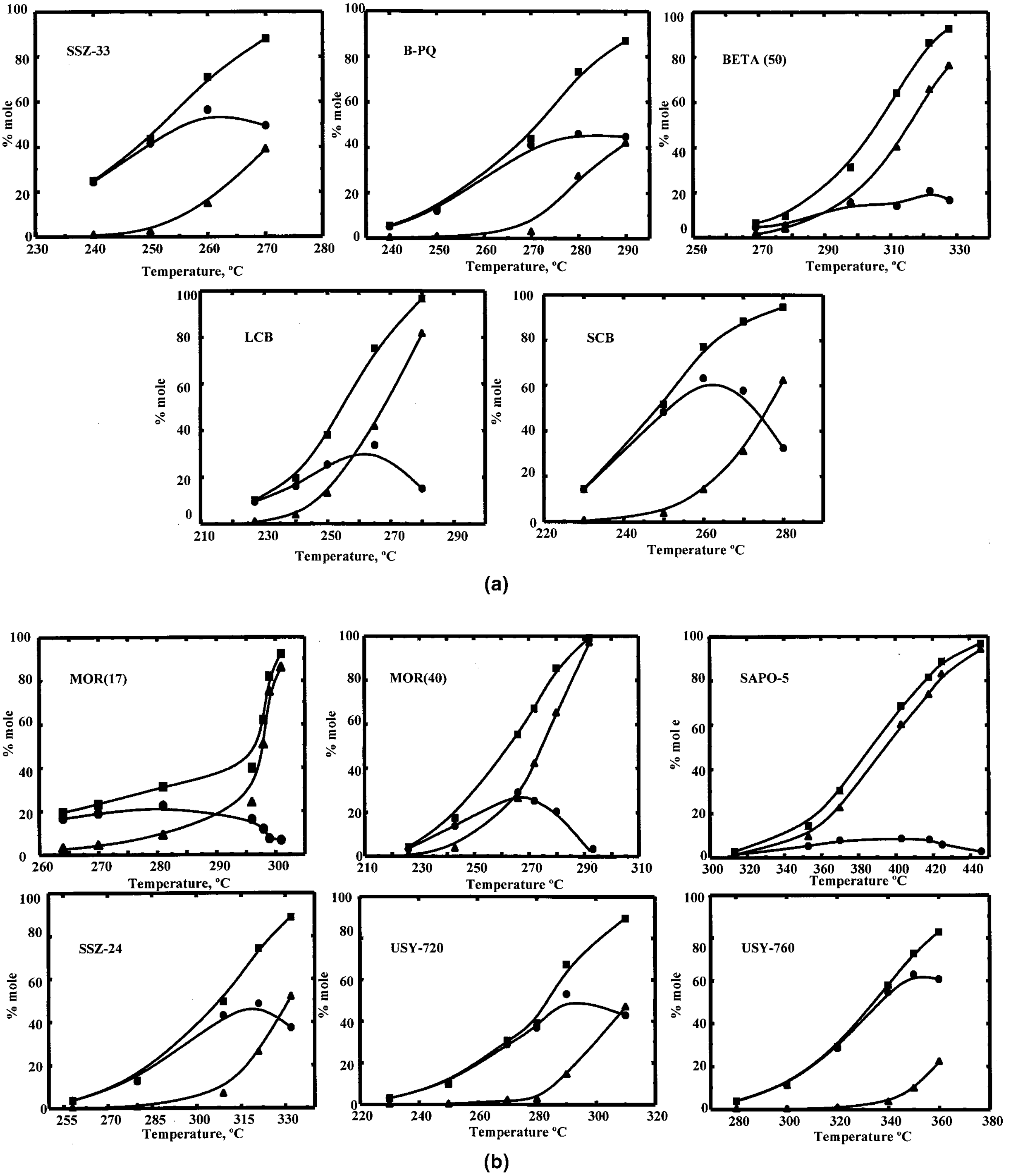

FIG. 4. Total conversion (■), isomerization (●), and cracking (▲) yields of *n*-heptane versus reaction temperature. Reaction conditions: 5.13 WHSV, 20 bar total pressure, and H_2/hydrocarbon ratio of 15 mol mol^{-1}. (a) SSZ-33, B-PQ, BETA (50), LCB, and SCB. (b) MOR (40), MOR, SAPO-5, SSZ-24, USY-720, and USY-760.

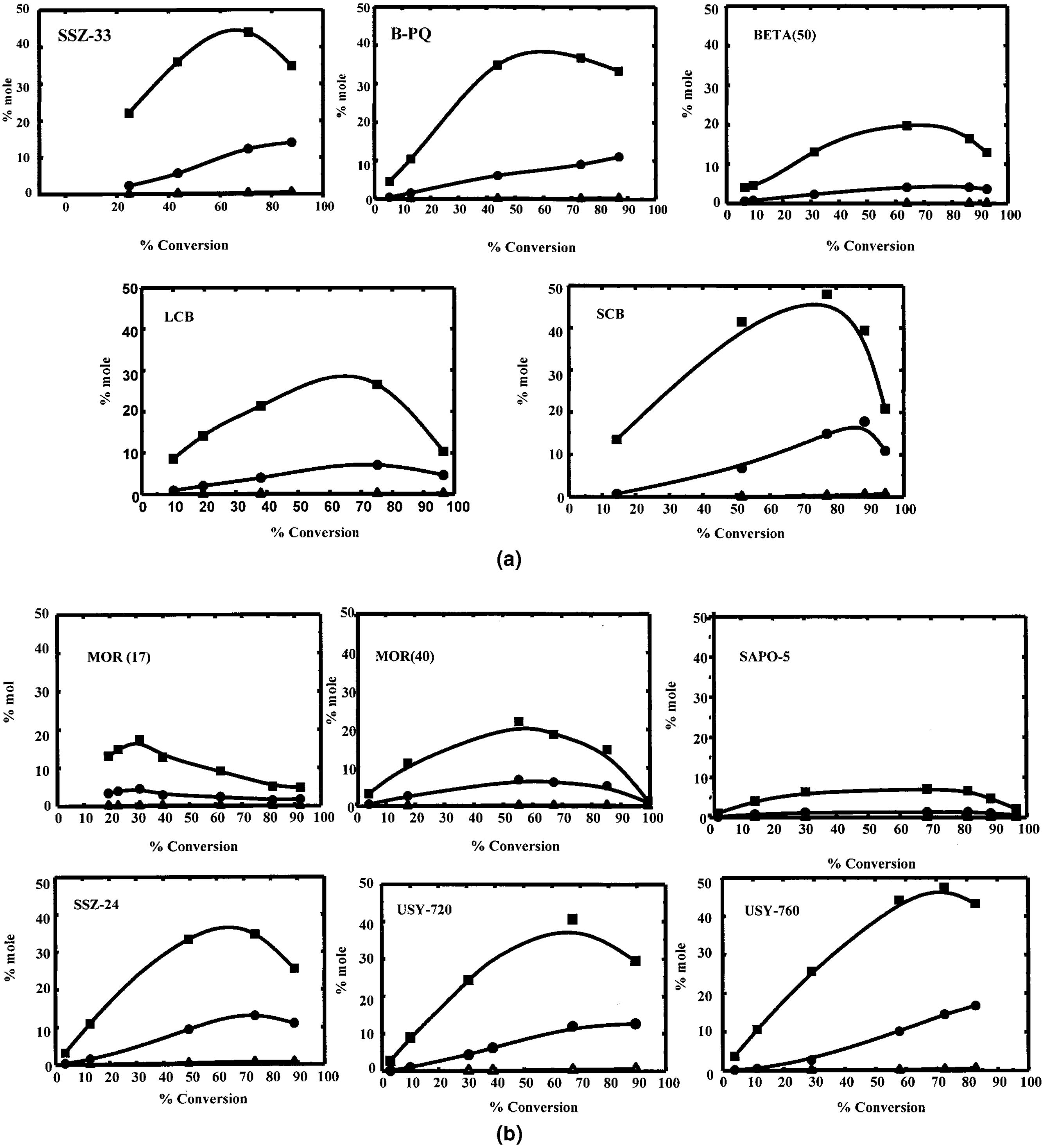

FIG. 5. Isomer distribution (monobranched (■), dibranched (●), and tribranched (▲)) versus conversion during *n*-heptane isomerization. Reaction conditions: 5.13 WHSV, 20 bar total pressure, and H_2/hydrocarbon ratio of 15 mol mol^{-1}. (a) SSZ-33, B-PQ, BETA(50), LBC, and SBC. (b) MOR, MOR (40), SAPO-5, SSZ-24, USY-720, and USY-760.

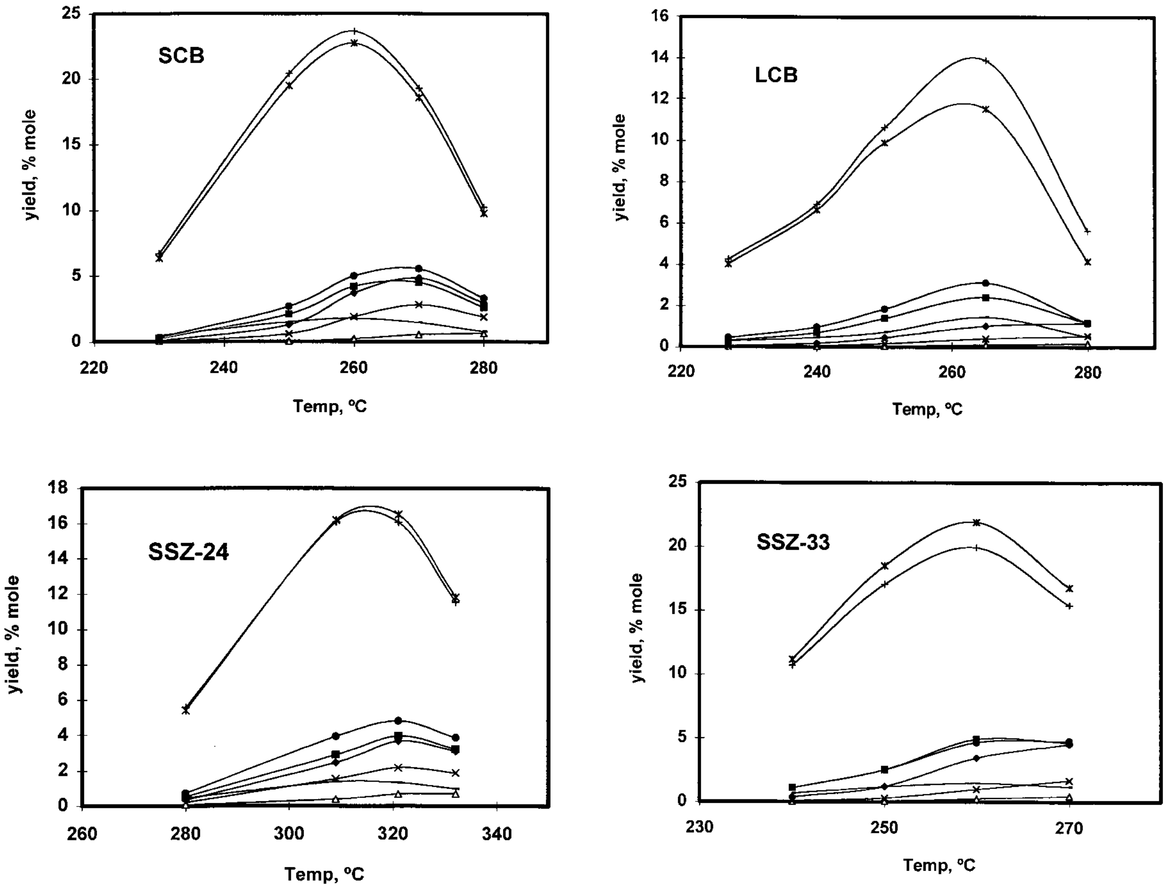

FIG. 6. Isomer distribution in the isomerization of *n*-heptane versus reaction temperature on different catalysts. The numbers in brackets are the Research Octane Numbers (RON) of each isomer: (◆) 2,2-DMP(98.2), (■) 2,4-DMP (83.1), (▲) 2,2,3-TMB (112), (×) 3,3-DMP (80.8), (∗) 2-MH (42.3), (●) 2,3-DMP (91.1), (+) 3-MH (52), and (−) 3-EP (65). Reaction conditions: 5.13 WHSV, 20 bar total pressure, and H_2/hydrocarbon ratio of 15 mol mol^{-1}.

isomerization catalyst. Indeed, when approaching the equilibrium conversion the selectivity to isomerization is above 98%. From the point of view of activity, the nanocrystalline Beta zeolite is at least as active as the optimized H-mordenite. These results, and those obtained for the hydroisomerization of *n*-heptane on the nanocrystalline Beta zeolite, were encouraging for the possibilities of this material for carrying out the hydroisomerization of LSR feeds containing larger concentrations of *n*-hexane and *n*-heptane (*n*-hexane : *n*-pentane : *n*-heptane equal to 3 : 1 : 1 molar ratio). This possibility has been studied further by reacting the second LSR feed on the optimized H-mordenite and on the nanocrystalline Beta zeolite.

The results given in Fig. 8 clearly show that regardless of the zeolite used the reactivity follows the order *n*-heptane > *n*-hexane > *n*-pentane, as could be expected taking into account the heats of adsorption of the different hydrocarbons (20). Moreover, it is also clear that the nanocrystalline Beta zeolite is more active and selective than H-mordenite for the isomerization of *n*-hexane and *n*-heptane. Indeed, while *n*-pentane is hardly cracked on any of the two zeolites, in the case of *n*-hexane it is possible to reach ~80% conversion with ~96% selectivity on the Beta sample, while at the same level of conversion the selectivity to isomerization on H-mordenite is lower than 88%. The selectivity differences are much more notorious in the case of *n*-heptane, which readily cracks on H-mordenite, while for the Beta sample the isomerization selectivity is high until reaching ~75% conversion.

When the isomerization of the different components is considered globally, one can see that, even on the nanocrystalline Beta (Fig. 8), under the conditions necessary to obtain high levels of conversions of *n*-pentane and *n*-hexane, *n*-heptane is already extensively cracked (see, for instance, the results obtained at ~280°C). Nevertheless, it is possible to conclude that for LSR containing significant amounts of *n*-heptane, a nanocrystalline zeolite will be a better catalyst option than mordenite. Indeed, when using mordenite as a catalyst, practically all heptane will be cracked, with the corresponding consumption of hydrogen and possible coke formation, while on the nanocrystalline Beta zeolite 50% of the total heptane converted will remain as branched

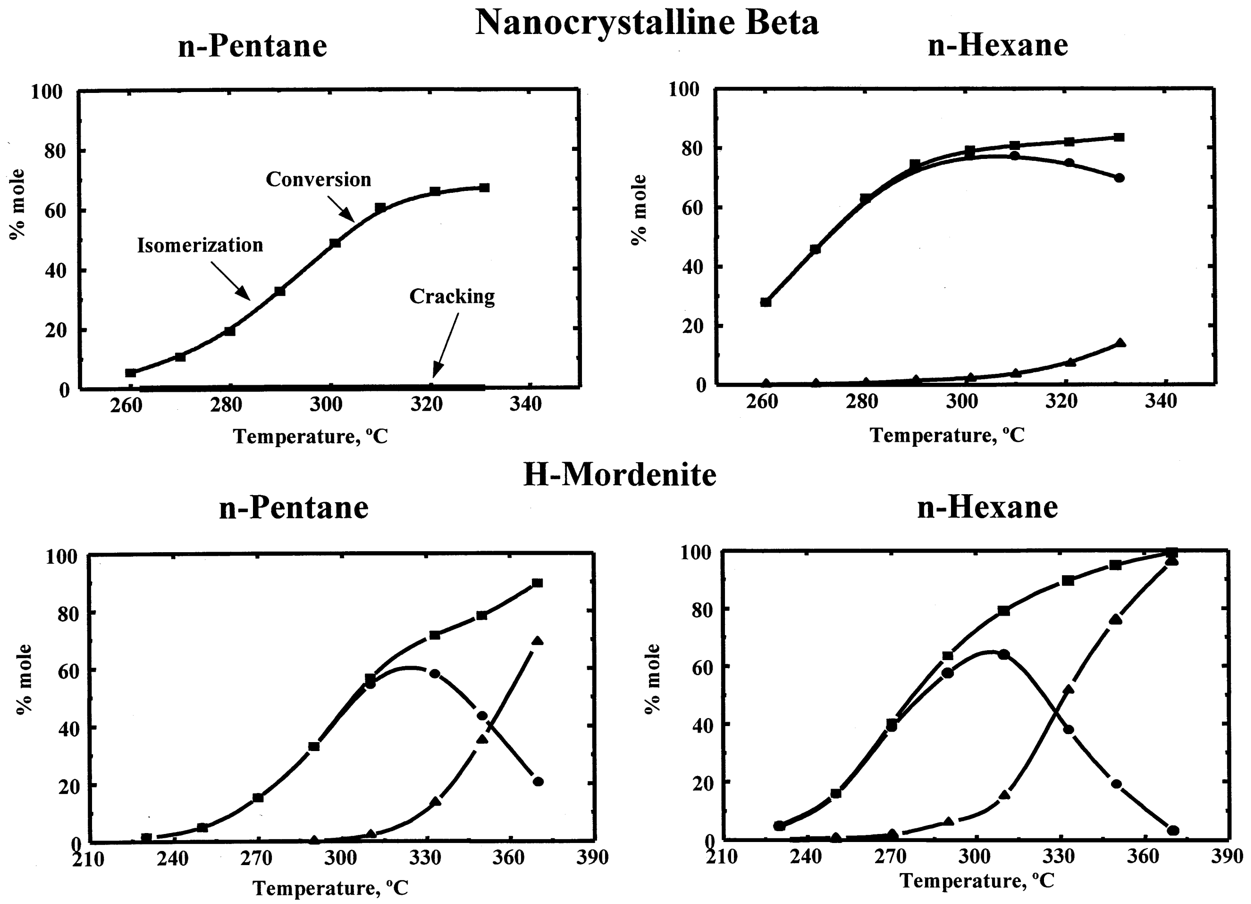

FIG. 7. Total conversion (■), isomerization (●), and cracking (▲) yields of *n*-pentane and *n*-hexane versus reaction temperature. Reaction conditions: 5.13 WHSV, 20 bar total pressure, and H_2/hydrocarbon ratio of 15 mol mol^{-1}.

isomers in a ratio of mono- : di- : tri- products of 4 : 1 : 0.1 (see Fig. 9). However, taking into account that the level of conversion was varied by varying the reaction temperature, differences may exist between the activation energies for isomerization and cracking, especially in the case of highly branched isomers. Therefore, we have also performed additional work in which the level of conversion was changed by modifying the contact time while the reaction temperature was kept constant at 270°C. The results presented in Fig. 10 show that the observed selectivities are only a function of the level of conversion, and therefore the above discussion is still valid regardless of the reaction conditions used.

4. CONCLUSIONS

The hydroisomerization of *n*-heptane to high octane dibranched and tribranched products has been studied using a commercial type of LSR isomerization catalyst, i.e., mordenite, as well as on other uni- and tridirectional 12 MR and 10 × 12 MR zeolites. Mordenite cracks *n*-heptane products very quickly, giving low selectivities to branched products. While a larger unidirectional pore zeolite (SSZ-24) gives better results than H-mordenite, the 12 MR tridirectional zeolites are the best catalysts for the branching isomerization of *n*-heptane, owing to the faster diffusion rates of reactants and products through the micropores. The zeolite crystal size has been found to be of paramount importance, because the catalytic activity and selectivity of a nanocrystalline Beta zeolite was better than that of Beta zeolites with larger crystallites.

When nanocrystalline Beta samples were used for converting a LSR formed by *n*-pentane and *n*-hexane its behaviour was even better than that of an optimized commercial-type mordenite zeolite catalyst. The advantage of the nanocrystalline Beta zeolite is even greater when it is used for the isomerization of an LSR feed also containing *n*-heptane (20 wt%). While mordenite gives a complete cracking of the *n*-heptane present in the feed, the nanocrystalline Beta cracks only 50% and the other 50% of the converted *n*-heptane is present as branched C_7 products with a ratio of mono : di : tri isomers of 4 : 1 : 0.1. This higher selectivity of the nanocrystalline Beta zeolite is important not only with respect to the volume yield but also with respect to H_2 consumption and coke formation.

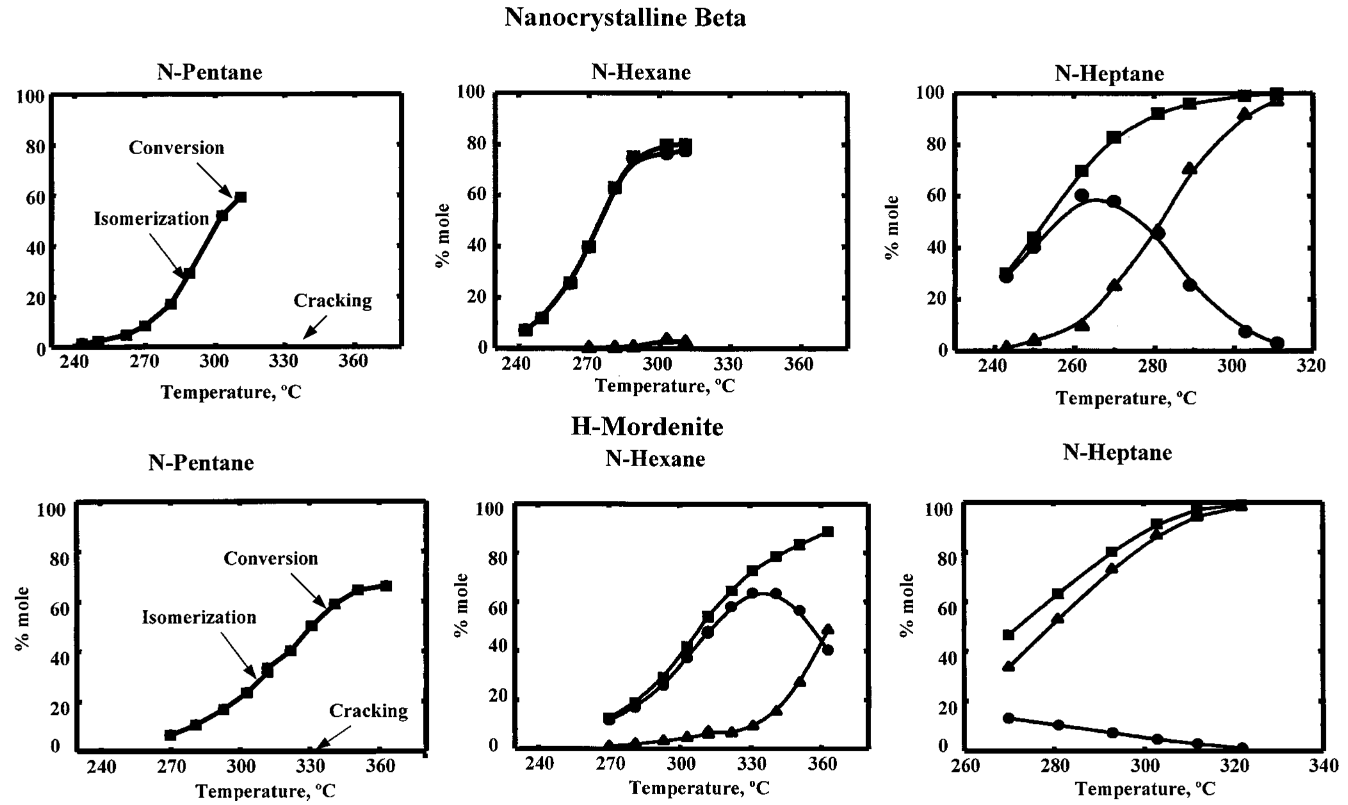

FIG. 8. Total conversion, isomerization, and cracking yields of *n*-pentane, *n*-hexane, and *n*-heptane versus reaction temperature. Reaction conditions: 5.13 WHSV, 20 bar total pressure, and H_2/hydrocarbon ratio of 15 mol mol^{-1}.

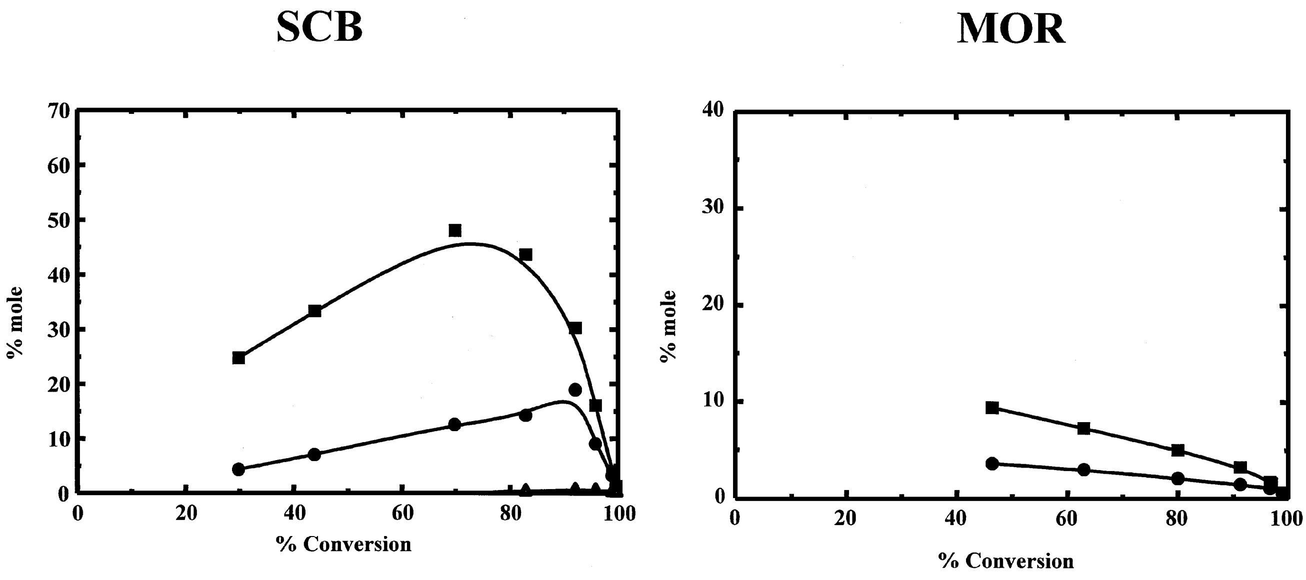

FIG. 9. Isomer distribution during *n*-heptane isomerization over SCB and MOR: (■) monobranched, (●) dibranched and (△) tribranched. Reaction conditions: 5.13 WHSV, 20 bar total pressure, and H_2/hydrocarbon ratio of 15 mol mol^{-1}.

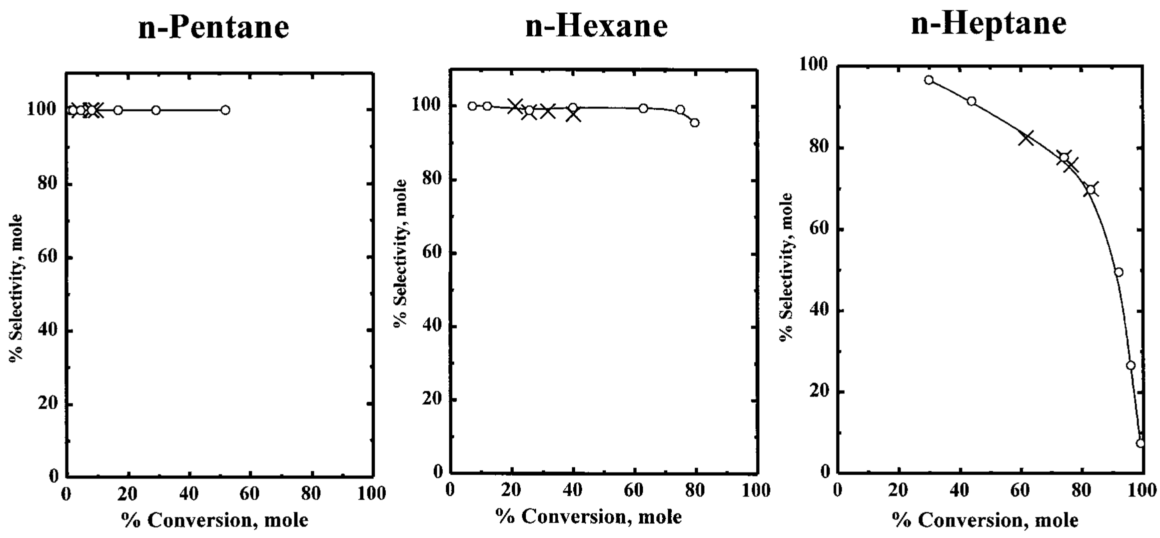

FIG. 10. Selectivities to isomerization. (○) Data obtained at constant contact time (0.197 h^{-1}) and different temperatures. (×) Data obtained at constant temperature (270°C) and different contact times.

ACKNOWLEDGMENT

Financial support by the Spanish Comisión Interministerial de Ciencia y Tecnología, CICYT, (Proyect MAT 97-1016-C02-01) is gratefully acknowledged.

REFERENCES

1. Asselin, G. F., Bloch, H. S., Donaldson, G. R., Haensel, V., and Pollitzer, E. L., "Symposium on Advances in Gasoline Technology." ACS, New York, Aug. 27, 1972.
2. Kouwenhoven, H. W., and Van Zijll Langhout, W. X., *Chem. Eng. Proc.* **67**(4), 65 (1971).
3. Steinberg, K. H., Becker, K., and Nestler, K. H., *Acta Phys. Chim.* **31**(1–2), 44 (1985).
4. Spivey, J. P., and Bryant, P. A., *Ind. Eng. Chem. Prod. Res. Dev.* **11**, 3 (1972).
5. Corma, A., Lázaro, J. J., and Frontela, M. J., U.S. Patent 5,057,471 (1989).
6. Corma, A., Frontela, J., Lazaro, J., and Perez, M., *ACS Petrol. Div.* **36**, 883 (1991).
7. Van Nordtrand, V. A., Santilli, D. N., and Zones, S. L., *in* "Molecular Sieves: Synthesis of Microporous Material" (M. L. Occelli and H. Robson, Eds.), p. 373, 1992.
8. Lok, B. M., Messina, C. A., Patton, R. L., Gajek, R. T., Cannan, T. R., and Flanigen, E. M., U.S. Patent 4440871, 1984.
9. Zones, S. L., U.S. Patent 4963337, Chevron Research Co., 1990.
10. Camblor, M. A., Corma, A., Mifsud, A., Perez-Pariente, J., and Valencia, S., *Stud. Surf. Sci. Catal.* **105**, 341 (1997).
11. Camblor, M. A., Corma, A., and Valencia, S., *J. Mater. Chem.* **8**(9), 2137–2145 (1998).
12. Corma, A., Fornés, V., Martinez, A., and Orchillés, A. V., *in* "Perspectives in Molecular Sieves Science" (W. H. Flank and T. E. Whyle, Jr., Eds.), ACS Symp. Ser., Vol. 368, p. 542. Am. Chem. Soc., Washington, DC, 1988.
13. Mirodatos, C., and Barthomeuf, D., *J. Chem. Soc. Chem. Commun.* **39**, (1981).
14. Bertolacini, R. J., U.S. Patent 4018711, 1977.
15. Fichtner-Schmitter, H., Lose, U., Engelhardt, G., and Patzelova, V., *Cryst. Res. Technol.* **19**, K1–K2 (1984).
16. Weitkamp, J., Engelhardt, W., and Jacobs, P. A., *Acta Phys. Chem.* **31**, 261 (1985).
17. Martens, J. A., Tielen, M., and Jacobs, P. A., *Stud. Surf. Sci. Catal.* **46**, 49 (1989).
18. Lobo, R. F., and Davis, M. E., *J. Am. Chem. Soc.* **117**, 3764 (1995).
19. Martens, J. A., Jacobs, P. A., and Weitkamp, J., *Appl. Catal.* **20**, 239–281 (1986).
20. Haag, W. O., *in* "Abstracts of Papers of the American Chemical Society," Vol. 211, Iss. MAR, pp. 6-PTR, 1996. [UA485]